Jpn J Radiol (2012) 30:255–262
DOI 10.1007/s11604-011-0041-8

ORIGINAL ARTICLE

Fused 99m-Tc-GSA SPECT/CT imaging for the preoperative evaluation of postoperative liver function: can the liver uptake index predict postoperative hepatic functional reserve?

Morikatsu Yoshida · Shinya Shiraishi · Fumi Sakaguchi · Daisuke Utsunomiya · Kuniyuki Tashiro · Seiji Tomiguchi · Hirohisa Okabe · Toru Beppu · Hideo Baba · Yasuyuki Yamashita

Received: 12 October 2011 / Accepted: 3 December 2011 / Published online: 3 February 2012

Abstract
Purpose To evaluate the role of hepatic asialoglycoprotein receptor analysis in the preoperative estimation of postoperative hepatic functional reserve.
Methods We obtained technetium-99m-diethylenetriaminepentaacetic acid-galactosyl human serum albumin (99mTc-GSA) SPECT/CT fusion images in 256 patients with liver disease scheduled for hepatic resection. The liver uptake value corrected for body surface area [$LUV_{(BSA)}$] and liver uptake ratio (LUR) of the remnant were preoperatively estimated based on the fused images. These values were compared with the postoperative hepatic functional reserve.
Results Significant correlations were observed between $LUV_{(BSA)}$, LUR, and most conventional indicators of hepatic functional reserve. Postoperatively, nonpreserved liver functional reserve was observed in 15 of the 256 patients (5.8%). Remnant $LUV_{(BSA)}$ showed better correlation than remnant LUR or the other indicators. No patients with remnant $LUV_{(BSA)}$ above 28.0 manifested poor nonpreserved functional reserve. Using a $LUV_{(BSA)}$ of 27.0, it was possible to predict postoperative poor hepatic functional reserve at a sensitivity of 91%, specificity of 81%, and accuracy of 81% postoperatively. According to multivariate analysis, a low remnant $LUV_{(BSA)}$ was the only significant independent predictor of poor hepatic functional reserve.
Conclusions Our 99mTc-GSA SPECT/CT fusion imaging method was clinically useful for evaluating regional hepatic function and for predicting postoperative hepatic functional reserve.

Keywords Fusion imaging · 99mTc-GSA SPECT · Computed tomography · Liver function · Liver resection

M. Yoshida (✉) · S. Shiraishi · F. Sakaguchi · D. Utsunomiya · Y. Yamashita
Department of Diagnostic Radiology, Faculty of Life Sciences, Kumamoto University, 1-1-1 Honjo, Kumamoto 860-8556, Japan
e-mail: y_morikatsu@hotmail.com

K. Tashiro
Kumamoto City Hospital, Kumamoto, Japan

S. Tomiguchi · H. Okabe · T. Beppu · H. Baba
Department of Diagnostic Radiology, School of Health Sciences, Kumamoto University, Kumamoto, Japan

S. Tomiguchi · H. Okabe · T. Beppu · H. Baba
Department of Gastroenterological Surgery, Faculty of Life Sciences, Kumamoto University, Kumamoto, Japan

Introduction

The evaluation, before major liver resection or living donor liver transplantation, of the future liver functional reserve of the remnant is crucial to identifying patients at increased risk for postoperative liver failure [1–6]. As extended hepatectomy is associated with higher operative morbidity and mortality rates, particularly in patients with parenchymal liver disease [7], preoperative evaluation of the function of the liver remnant is important for determining whether extended liver resection is safe.

To estimate hepatic functional reserve, 99mTc-labeled diethylene triamine pentaacetate-galactosyl human serum albumin (99mTc-GSA), a radiopharmaceutical that binds specifically to the hepatic asialoglycoprotein receptor (ASGP-R), is used to estimate hepatic function [8, 9]. Because ASGP-R is a natural superficial antigen of viable hepatocytes, the uptake of 99mTc-GSA is independent of biochemical processes, and allows the direct estimation of the functioning hepatocyte mass [10].

Using 99mTc-GSA scintigraphy imaging, many different parameters can be calculated from different kinetic models [11–15]. However, they are highly complex and thus not widely used in the context of liver surgery. The hepatic uptake ratio and the blood clearance ratio of 99mTc-GSA are the most commonly used parameters determined from planar dynamic 99mTc-GSA scintigraphs [10]. Because they do not incorporate regional functional differences into the included volume, the future function of the liver remnant cannot be estimated. With a SPECT/CT system, functional data from 99mTc-GSA SPECT images can be combined with the accurate anatomic information from CT scans [16]; using an arbitrary volume of interest, precise measurements of the regional accumulation and volume are possible. We acquired 99mTc-GSA SPECT/CT 3D fused images and investigated whether the liver uptake value (LUV), which reflects the amount of ASGPRs in the region of interest (ROI), could be used to accurately estimate the postoperative function of the liver remnant.

We evaluated the usefulness of the preoperative estimation of LUV in the remnant liver and analyzed the correlation between the preoperative LUV and the actual postoperative liver dysfunction.

Materials and methods

Patients

We retrospectively reviewed 99mTc-GSA SPECT/CT 3D fused images of 256 patients (199 males and 57 females, mean age 66.0 ± 10.0 years) who underwent systematic liver resection between January 2007 and January 2011 at the Department of Gastroenterological Surgery of our hospital. Of these, 197 presented with hepatocellular carcinoma, 40 with liver metastasis, 7 with intrahepatic cholangiocarcinoma, and 12 with other diseases. According to the International Hepato-Pancreato-Biliary Association classification [9, 17], 7 patients underwent segmentectomy, 65 monosectionectomy, 89 disectionectomy, and 5 trisectionectomy.

Informed consent was obtained from all patients before 99mTc-SPECT/CT examination.

SPECT/CT system

We used a combined SPECT/CT system with dual-head detectors and a 16-row MDCT scanner (Symbia T16, Siemens Healthcare, Erlangen, Germany). The two instruments were juxtaposed so that the CT table bearing the patient could be moved directly into the SPECT scanner for CT [16].

SPECT imaging

99mTc-GSA (185 MBq) was injected as a bolus into an antecubital vein. Dynamic scintigrams and SPECT images were obtained with the same gamma camera fitted with a low-to-medium energy general-purpose (LMEGP) collimator.

During dynamic scintigraphy, we acquired sequential anterior abdominal images (64 × 64 matrix) that included the heart and liver; these were taken at 20 s intervals for 18 min. The blood clearance index was calculated by dividing the radioactivity in the heart ROI at 15 min postinjection by the radioactivity of the heart ROI at 3 min (HH15). The receptor index was calculated by dividing the radioactivity of the liver ROI by the sum of the radioactivity of the liver and heart ROIs at 15 min postinjection (LHL15).

Hepatic SPECT data (60 steps of 15 s/step, 360°, 128 × 128 matrix) were obtained from 20 to 35 min after the dynamic scintigraphic study. We acquired 64 projections at 6° intervals in the continuous mode. For SPECT reconstruction, the ordered-subset expectation–maximization (OS-EM) algorithm was used (8 iterations, 6 subsets). Postprocessing was performed with a 7.8 mm Gaussian filter.

CT imaging and liver volumetry

We obtained noncontrast helical CT images of the abdomen for attenuation correction of the SPECT images with breath-hold under expiration; the imaging parameters were 120 kV, 50 mA, 17.5 mm table feed per rotation, 0.7 s gantry rotation time, 1.25 mm collimation, and 1.25 mm reconstruction. CT images were reconstructed with a standard reconstruction algorithm with a 50 cm field of view to cover both the patient and the table. Reconstructive CT images were processed into DICOM data.

For liver volumetry, each CT slice was analyzed as follows. The outline of the ROI was traced manually in each image section; the gall bladder, retrohepatic vena cava, and the main branches of the intrahepatic vascular structures were excluded. Using an automated process, all slices were stacked to build a virtual model of the liver. Volumetric values were obtained with inherent software and a volume-rendering algorithm. The total liver volume (TLV) excluding the tumor volume was measured. The model of the whole liver was then subjected to virtual hepatic resection based on the operative strategy applied in individual patients, and the volume of segments to be remnant and the residual liver volume (remnant LV) were measured. The relative resected liver volume (% remnant LV) was expressed as a percentage of TLV. In

cases where the type of resection actually performed differed from that planned preoperatively, volumetric analysis was repeated based on the actual surgical procedure.

Image processing

Fusion of the SPECT and CT images (slice thickness 2.5 mm) was performed semi-automatically via registration of the liver shape on a dedicated workstation on the SPECT/CT scanner. After image registration, a CT-derived attenuation-coefficient map was created. The SPECT images were then reconstructed with attenuation correction using the OS-EM algorithm (3 iterations, 8 subsets). The final step—fusion of the attenuation-corrected SPECT- and CT images—was performed on another dedicated workstation (Virtual Place Lexus, AZE, Tokyo, Japan). The TLV was also measured on CT images; the TLV without tumor masses was delineated manually based on the consensus of two board-certified radiologists, and summed for each acquisition.

Calculation of the SPECT parameters of the LUV

LUV was based on liver uptake ratio (LUR), defined as follows [18]:

$$\mathrm{LUR} = [\text{radioactivity (whole liver)}/\text{radioactivity (injected)}] \times 100.$$

To estimate hepatocyte function, we defined three LUV parameters by correcting for body weight (BW), liver volume (LV), and body surface area (BSA) as follows:

$$\mathrm{LUV}_{(\mathrm{BSA})} = \mathrm{LUR}/\mathrm{BSA}$$
$$\mathrm{LUV}_{(\mathrm{BW})} = \mathrm{LUR}/\mathrm{BW}$$
$$\mathrm{LUV}_{(\mathrm{LV})} = \mathrm{LUR}/\mathrm{LV}.$$

Before SPECT scanning, we measured the preinjection radioactivity in the syringe on a scintillation counter (ICG-7, Aloka, Tokyo, Japan). Using a premeasured calibration factor for a phantom, we converted the SPECT count of the whole liver into radioactivity values.

The resection line of the liver was determined through the consensus of a surgeon and a radiologist, based on the course of the hepatic portal and the hepatic vein on SPECT/CT fused images; the radioactivity obtained in the remnant liver was divided by the total preinjection radioactivity and corrected for BSA. The result was considered the LUV of the remnant. The relative residual liver function (% remnant LF) was calculated as follows:

$$\%\ \text{remnant LF} = \text{residual LUR}/\text{whole LUR}.$$

Table 1 Scoring of total serum bilirubin and prothrombin time

Score	0	1	2
Total serum bilirubin (mg/dl)	<2	2–3	>3
Prothrombin time (%)	>70	50–70	>50

Severity of hepatic dysfunction was classified based on the sum of the scores: none = 0, mild = 1, moderate = 2, severe = 3 or 4

Assessment of postoperative liver dysfunction and functional reserve

We defined postoperative hepatic dysfunction based on a combination of minimum prothrombin time (PT) and maximum total bilirubin (T-Bil) on postoperative day (POD) 5. It was graded as none, mild, moderate, or severe by summing the scores of PT and T-Bil (Table 1) [19, 20]. We divided the patients into two groups of postoperative hepatic functional reserve; preserved and nonpreserved. The nonpreserved group was defined as having moderate to severe hepatic dysfunction on POD 5, and the preserved group was defined as none or mild hepatic dysfunction on POD 5.

Statistical analysis

Statistical analysis was performed with the statistical software package JMP (version 9; SAS, Cary, NC, USA).

We performed a receiver operating characteristic (ROC) curve analysis to identify the values of remnant $\mathrm{LUV}_{(\mathrm{BSA})}$, remnant $\mathrm{LUV}_{(\mathrm{BW})}$, remnant $\mathrm{LUV}_{(\mathrm{LV})}$, and remnant LUR in order to predict nonpreserved functional reserve with a sensitivity of at least 90% and a specificity of not less than 80%.

Correlations between the LUR and $\mathrm{LUV}_{(\mathrm{BSA})}$ values and the results of each liver function test were subjected to standard Pearson correlation analysis. Correlations between the remnant LUR and remnant $\mathrm{LUV}_{(\mathrm{BSA})}$ values and T-Bil and PT on POD 5 were subjected to standard Pearson correlation analysis. One-way analysis of variance (ANOVA) was performed to assess differences in the remnant $\mathrm{LUV}_{(\mathrm{BSA})}$ between patients without and with hepatic dysfunction of various severities. The independent sample *t* test was used to examine differences in remnant $\mathrm{LUV}_{(\mathrm{BSA})}$ between patients without and with postoperative hepatic dysfunction of moderate to severe degrees and poor functional reserve. Univariate analysis of preoperative variables was performed with the Pearson chi-squared test, the Fisher exact test, and the independent sample *t* test. The Pearson chi-squared test was used for surgical procedure and the Fisher exact test was used for gender. The independent sample *t* test was used for other and continuous variables. Probability values of less than 0.05 were

considered statistically significant. Significant variables in univariate analysis were entered simultaneously (forced entry method) into the multivariate logistic regression to evaluate their independent predictive values for hepatic functional reserve.

Results

ROC curve analysis of remnant LUV to predict postoperative functional reserve

The ROC curves of remnant $LUV_{(BSA)}$, remnant $LUV_{(BW)}$, remnant $LUV_{(LV)}$, and remnant LUR, used to predict postoperative nonpreserved hepatic functional reserve, are shown in Fig. 1. The AUCs of the remnant $LUV_{(BSA)}$, remnant $LUV_{(BW)}$, remnant $LUV_{(LV)}$, and remnant LUR were 0.89, 0.85, 0.73, and 0.87, respectively. Using 27.0 for $LUV_{(BSA)}$, it was possible to predict postoperative nonpreserved hepatic reserve with a sensitivity of 91%, specificity of 81%, and accuracy of 81%. Positive and negative predictive values were 31 and 99%, respectively. The likelihood ratios for nonpreserved and preserved hepatic functional reserve were 4.6 and 8.8, respectively. Results of all indices are shown Table 2. Remnant $LUV_{(BSA)}$ was the most accurate index for predicting postoperative functional reserve. Therefore, we adopted $LUV_{(BSA)}$ for further evaluations. A remnant $LUV_{(BSA)}$ of 27.0 or less was statistically significantly associated with nonpreserved postoperative hepatic functional reserve.

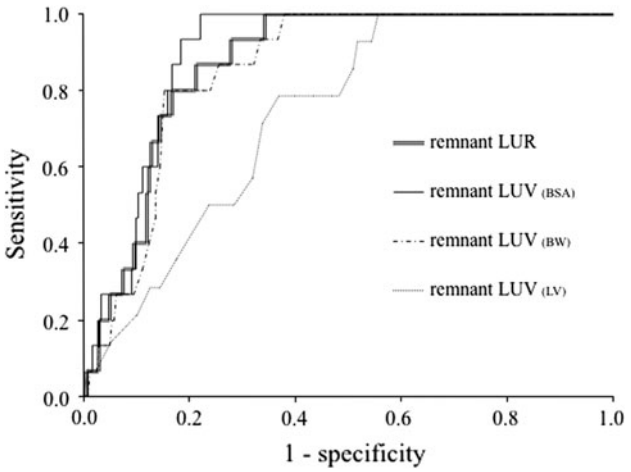

Fig. 1 Receiver operating characteristic curve analysis of $LUV_{(BSA)}$, $LUV_{(BW)}$, $LUV_{(LV)}$, and LUR of the remnant, as used to predict postoperative non-preserved hepatic functional reserve

Correlations between 99mTc-GSA SPECT and conventional liver function tests

Correlations between liver function tests and $LUV_{(BSA)}$ and LUR are shown in Table 3. There were significant correlations between $LUV_{(BSA)}$ and most of the conventional indicators of hepatic functional reserve, including indocyanine green retention rate at 15 min (ICG-R15), albumin level, aspartate aminotransferase (AST), alanine aminotransferase (ALT), cholinesterase activity (ChE), prothrombin time, platelet counts, serum hyaluronic acid, HH15, and LHL15. LUR values for the whole liver were also significantly correlated with the results of most of the

Table 3 Correlation between conventional liver functional tests and indices from 99mTc-GSA SPECT

	$LUV_{(BSA)}$(R)	LUR(R)
Bilirubin (mg/dl)	−0.09	0.001
Albumin (g/dl)	0.15*	0.19*
AST (IU/l)	−0.22*	−0.31**
ALT (IL/l)	−0.21*	−0.23*
GGT (IU/l)	−0.02	−0.01
Cholinesterase (U/l)	0.18*	0.30**
Cholesterol (mg/dl)	0.12	0.11
Platelets ($\times 10^4/mm^3$)	0.40**	0.44**
PT (%)	0.33**	0.30**
Serum hyaluronic acid (ng/ml)	−0.29**	−0.47**
ICG R15 (%)	−0.48**	−0.47**
HH15	−0.60**	−0.73**
LHL15	0.54**	0.67**

AST aspartate aminotransferase, *ALT* alanine aminotransferase, *GGT* glutamyltranspeptidase, *PT* prothrombin time

* $P < 0.05$, ** $P < 0.0001$

Table 2 Diagnostic performances of four indices for predicting postoperative functional reserve

	Cut off	Sensitivity (%)	Specificity (%)	Accuracy (%)	PPV (%)	NPV (%)
$rLUV_{(BSA)}$	27.0	91	81	81	31	99
rLUR	50.0	93	66	67	15	99
$rLUR_{(BW)}$	0.66	80	84	85	24	99
$rLUR_{(LV)}$	0.21	92	46	45	10	99

rLUV$_{(BSA)}$ remnant $LUV_{(BSA)}$, *rLUR* remnant LUR, *rLUR*$_{(BW)}$ remnant $LUR_{(BW)}$, *rLUR*$_{(LV)}$ remnant $LUR_{(LV)}$, *PPV* positive predictive value, *NPV* negative predictive value

conventional liver function tests, including ICG R15, albumin levels, AST, ALT, cholinesterase activity, prothrombin time, and platelet counts, serum hyaluronic acid, HH15, and LHL15.

Relationship among remnant LUV and remnant LUR and postoperative hepatic dysfunction and functional reserve

Correlations of remnant $LUV_{(BSA)}$ and LUR with PT and T-Bil on POD 5 are shown in Fig. 2. There were significant correlations of remnant $LUV_{(BSA)}$ and remnant LUR with PT and T-Bil on POD 5. The correlation of remnant LUR with PT and T-Bil on POD 5 was better than that of remnant LUR with PT and T-Bil on POD 5.

No, mild, and moderate-to-severe hepatic dysfunction were observed in 201 (79%), 40 (16%), and 15 (6%) on POD5. The mean $LUV_{(BSA)}$ and the LUR of the remnant were significantly higher in patients without than with mild hepatic dysfunction on POD5 (34.7 ± 7.5 vs. 28.6 ± 7.5, $P < 0.001$ and 55.5 ± 12.5 vs. 47.9 ± 10.9, $P < 0.001$). Patients with mild hepatic dysfunction on POD5

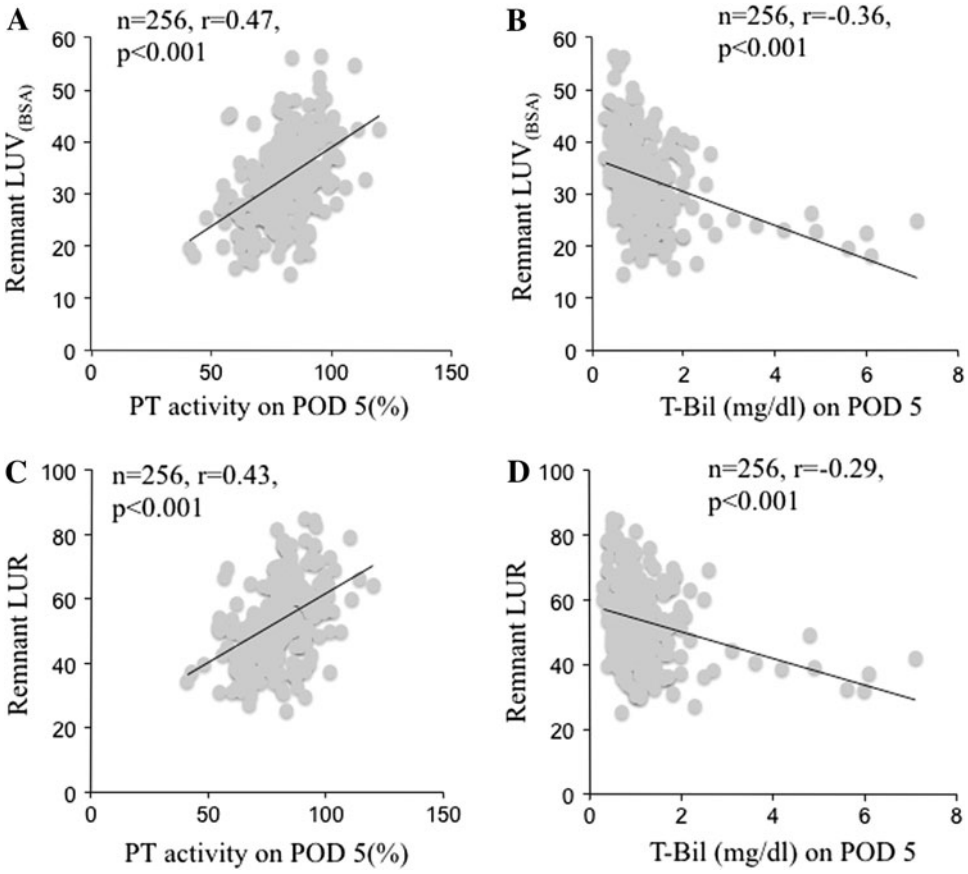

Fig. 2 Correlation of remnant $LUV_{(BSA)}$ (**a**, **b**) and LUR (**c**, **d**) with hepatic function on POD 5

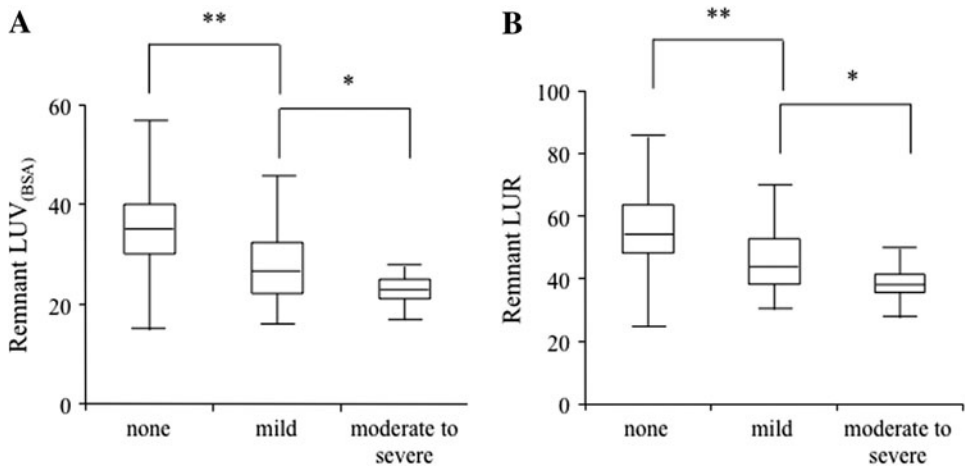

Fig. 3 Residual $LUV_{(BSA)}$ and LUR on POD5 in patients with no, mild, and moderate-to-severe hepatic dysfunction after liver resection. $^{**}P < 0.001$, $^{*}P < 0.05$

manifested a significantly higher mean remnant $LUV_{(BSA)}$ than did patients with moderate-to-severe hepatic dysfunction (28.6 ± 7.5 vs. 23.0 ± 3.1, $P < 0.05$ and 47.9 ± 10.9 vs. 38.8 ± 5.8, $P < 0.05$) (Fig. 3a, b).

Preoperative parameters to predict postoperative hepatic functional reserve

Univariate analysis showed that a small remnant $LUV_{(BSA)}$ ($P < 0.001$), a small % remnant LV ($P < 0.05$), a small % remnant LF ($P < 0.001$), and a high HH15 ($P < 0.001$) were significant predictors of nonpreserved hepatic functional reserve after liver resection (Table 4). When we entered the $LUV_{(BSA)}$ of the remnant, the % remnant LV, the % remnant LF, and HH15 into a multivariate logistic regression model to identify variables with independent predictive value for nonpreserved hepatic reserve, we found that a small remnant $LUV_{(BSA)}$ was the only significant independent predictor (Table 5). Seven of the 15 (47%) patients with nonpreserved hepatic reserve died perioperatively, which was defined as death within 30 days or during the hospital stay following surgery, whereas this was the case in 0 of the 241 without nonpreserved hepatic reserve ($P < 0.001$) (Table 6).

Discussion

Liver resection continues to carry risks for postoperative complications. The overall incidence of complications increases with the extent of liver resection [21, 22]. Key to improving the safety of liver resection is predicting hepatic functional reserve of the postoperative liver remnant. There is no evidence that leaving at least one-third of the healthy liver helps to avoid significant hepatic dysfunction, and the adequacy of the liver-remnant volume has been gauged largely via guesswork or crude measurements.

ASGP-R is present only on mammalian hepatocytes [23]. A significant decrease in ASGP-R and a concomitant increase in the accumulation of plasma asialoglycoproteins are seen in patients with impaired liver function [24, 25], and parameters obtained from planar 99mTc-GSA scintigraphy are valuable for the assessment of liver function [26–28]. We adopted a new index for $LUV_{(BSA)}$ that utilized not only SPECT but also CT images. Our SPECT/CT fused images yielded precise anatomical information on the $LUV_{(BSA)}$. Moreover, our functional imaging data were corrected for attenuation based on MDCT images. Seo et al. [29] showed that the quantification of SPECT images that were corrected for attenuation with CT images was more accurate than performing this quantification without attenuation correction. Yomoto et al. [30] reported that the amount of ASGP-R in the future liver remnant could be calculated correctly before surgery by using fused 99mTc-GSA SPECT and CT images; an accurate resection line could be drawn on the SPECT scans based on anatomical information yielded by the CT scans.

Table 4 Univariate analysis of variables predictive of hepatic functional reserve after liver resection

Parameters	Hepatic functional reserve		*P* value
	Preserved	Nonpreserved	
Gender (male:female)	185:56	14:1	0.20
Age	66.0 ± 10.3	64.3 ± 7.0	0.67
Surgical procedure (major:minor)	152:82	10:12	0.069
ICG R15 (%)	13.2 ± 6.9	16.1 ± 9.7	0.13
Serum albumin (g/dl)	3.96 ± 0.48	3.96 ± 0.31	0.98
Total serum bilirubin (mg/dl)	0.82 ± 0.3	0.95 ± 0.3	0.14
Serum cholinesterase activity	237.0 ± 76.5	206 ± 97.0	0.13
Serum hyaluronic acid (ng/ml)	128.3 ± 137.4	182.2 ± 157.6	0.19
Platelets ($\times 10^4/mm^3$)	16.0 ± 6.7	14.4 ± 6.0	0.38
PT (%)	94.8 ± 14.0	95.2 ± 12.5	0.90
Remnant $LUV_{(BSA)}$	33.6 ± 7.8	23.0 ± 3.1	<0.001
% remnant LV	73.7 ± 16.3	61.5 ± 17.0	<0.05
% remnant LF	75.3 ± 14.6	60.9 ± 13.3	<0.001
HH15	0.60 ± 0.07	0.64 ± 0.07	<0.05
LHL15	0.91 ± 0.03	0.90 ± 0.03	0.23

Table 5 Multivariate logistic regression analysis of variables predictive of nonpreserved hepatic functional reserve after liver resection

	Wald	Exp (*B*)	95% CI for Exp (*B*)	*P* value
HH15	0.70	0.017	1.16×10^{-6}–256.7	0.40
Remnant $LUV_{(BSA)}$	7.51	1.21	1.06–1.40	<0.001
% remnant LV	0.07	1.00	0.94–1.07	0.79
% remnant LF	0.01	1.00	0.93–1.08	0.89

Table 6 Relation of hepatic functional reserve to perioperative death

Died perioperatively	Nonpreserved hepatic reserve	
	No (%)	Yes (%)
No	241 (100)	8 (53)
Yes	0 (0)	7 (47)

Our method consisted of the fusion of attenuation-corrected SPECT and high-resolution CT images, and provided a more accurate estimate of the volume of the future liver remnant. We found that the combined assessment of 99m-Tc-GSA SPECT and CT images yielded more accurate information than calculating the relative RLV based on CT volumetry and other conventional parameters for predicting postoperative hepatic functional reserve. Therefore, we suggest that surgery can be performed safely in patients whose $LUV_{(BSA)}$ of the liver remnant is above 28.0. Although there was an overlap in the $LUV_{(BSA)}$ between patients with and without postoperative hepatic functional reserve, patients with larger $LUV_{(BSA)}$ usually showed good hepatic functional reserve following surgery. Surgery can be performed safely in patients whose $LUV_{(BSA)}$ of the liver remnant is above 28.0.

Sugahara et al. [18] found the LUR obtained from SPECT images was clinically useful for assessing the hepatic function of patients with chronic liver disease [31]. On the other hand, other studies have shown that body habitus may affect the postoperative complication rate [32, 33]. Therefore, we introduced a new index, $LUV_{(BSA)}$, which enabled a combined evaluation of the LUR and the patient's body habitus (BSA). Our results demonstrated that $LUV_{(BSA)}$ was superior to LUR, $LUV_{(BW)}$, and $LUV_{(LV)}$ for predicting the postoperative hepatic functional reserve. We believe that preoperative evaluation of the liver function should be performed with $LUV_{(BSA)}$.

Our study has several limitations. First, its design is retrospective, and it is a single academic center study. Our study population had only a few cases with nonpreserved liver functional reserve (16/256). Our results should therefore be confirmed by prospective and multicenter studies. Second, combined SPECT/CT systems are not widely used for attenuation correction because they are expensive and because they expose patients to additional radiation. Third, we drew the resection line on plain rather than contrast-enhanced CT images. However, the principal and portal veins for determining the resection line could be identified in all our patients. Lastly, we did not consider prolonged operating time, significant blood loss [34], diabetes mellitus [35], and chronic renal failure to be risk factors for postoperative liver dysfunction. Combined consideration of the $LUV_{(BSA)}$ of the liver remnant and these factors may yield a more accurate prediction of postoperative hepatic functional reserve.

In conclusion, assessment of the postoperative liver remnant on 99mTc-GSA SPECT/CT 3D fusion images is clinically useful for predicting postoperative dysfunction and hepatic functional reserve, and may aid in the selection of appropriate treatments and management strategies in patients with liver tumors.

References

1. Hwang EH, Taki J, Shuke N, Nakajima K, Kinuya S, Konishi S, et al. Preoperative assessment of residual hepatic functional reserve using 99mTc-DTPA-galactosyl-human serum albumin dynamic SPECT. J Nucl Med. 1999;40(10):1644–51.
2. Kokudo N, Vera DR, Koizumi M, Seki M, Sato T, Stadalnik RC, et al. Recovery of hepatic asialoglycoprotein receptors after major hepatic resection. J Nucl Med. 1999;40(1):137–41.
3. Mitsumori A, Nagaya I, Kimoto S, Akaki S, Togami I, Takeda Y, et al. Preoperative evaluation of hepatic functional reserve following hepatectomy by technetium-99m galactosyl human serum albumin liver scintigraphy and computed tomography. Eur J Nucl Med. 1998;25(10):1377–82.
4. Stadalnik RC, Vera DR, Woodle ES, Trudeau WL, Porter BA, Ward RE, et al. Technetium-99m NGA functional hepatic imaging: preliminary clinical experience. J Nucl Med. 1985; 26(11):1233–42.
5. Kubota K, Makuuchi M, Kusaka K, Kobayashi T, Miki K, Hasegawa K, et al. Measurement of liver volume and hepatic functional reserve as a guide to decision-making in resectional surgery for hepatic tumors. Hepatology. 1997;26(5):1176–81.
6. Kwon AH, Matsui Y, Kaibori M, Ha-Kawa SK. Preoperative regional maximal removal rate of technetium-99m-galactosyl human serum albumin (GSA-Rmax) is useful for judging the safety of hepatic resection. Surgery. 2006;140(3):379–86.
7. Madoff DC, Hicks ME, Vauthey JN, Charnsangavej C, Morello FA Jr, Ahrar K, et al. Transhepatic portal vein embolization: anatomy, indications, and technical considerations. Radiographics. 2002;22(5):1063–76.
8. Matsuzaki S, Onda M, Tajiri T, Kim DY. Hepatic lobar differences in progression of chronic liver disease: correlation of asialoglycoprotein scintigraphy and hepatic functional reserve. Hepatology. 1997;25(4):828–32.
9. Kudo M, Todo A, Ikekubo K, Hino M. Receptor index via hepatic asialoglycoprotein receptor imaging: correlation with chronic hepatocellular damage. Am J Gastroenterol. 1992;87(7):865–70.
10. Kwon AH, Ha-Kawa SK, Uetsuji S, Kamiyama Y, Tanaka Y. Use of technetium 99m diethylenetriamine-pentaacetic acid-galactosyl-human serum albumin liver scintigraphy in the evaluation of preoperative and postoperative hepatic functional reserve for hepatectomy. Surgery. 1995;117(4):429–34.
11. Vera DR, Stadalnik RC, Trudeau WL, Scheibe PO, Krohn KA. Measurement of receptor concentration and forward-binding rate constant via radiopharmacokinetic modeling of technetium-99m-galactosyl-neoglycoalbumin. J Nucl Med. 1991;32(6):1169–76.
12. Ha-Kawa SK, Tanaka Y. A quantitative model of technetium-99m-DTPA-galactosyl-HSA for the assessment of hepatic blood flow and hepatic binding receptor. J Nucl Med. 1991;32(12):2233–40.
13. Miki K, Kubota K, Kokudo N, Inoue Y, Bandai Y, Makuuchi M. Asialoglycoprotein receptor and hepatic blood flow using technetium-99m-DTPA-galactosyl human serum albumin. J Nucl Med. 1997;38(11):1798–807.
14. Shuke N, Okizaki A, Kino S, Sato J, Ishikawa Y, Zhao C, et al. Functional mapping of regional liver asialoglycoprotein receptor amount from single blood sample and SPECT. J Nucl Med. 2003;44(3):475–82.
15. Kaibori M, Ha-Kawa SK, Ishizaki M, Matsui K, Saito T, Kwon AH, et al. HA/GSA-Rmax ratio as a predictor of postoperative liver failure. World J Surg. 2008;32(11):2410–8.
16. Beppu T, Hayashi H, Okabe H, Masuda T, Mima K, Otao R, et al. Liver functional volumetry for portal vein embolization using a newly developed (99m)Tc-galactosyl human serum albumin scintigraphy SPECT-computed tomography fusion system. J Gastroenterol. 2011;46(7):938–43

17. Slankamenac K, Breitenstein S, Held U, Beck-Schimmer B, Puhan MA, Clavien PA. Development and validation of a prediction score for postoperative acute renal failure following liver resection. Ann Surg Clin Trial Valid Stud. 2009;250(5):720–8.
18. Sugahara K, Togashi H, Takahashi K, Onodera Y, Sanjo M, Misawa K, et al. Separate analysis of asialoglycoprotein receptors in the right and left hepatic lobes using Tc-GSA SPECT. Hepatology. 2003;38(6):1401–9.
19. Balzan S, Belghiti J, Farges O, Ogata S, Sauvanet A, Delefosse D, et al. The "50–50 criteria" on postoperative day 5: an accurate predictor of liver failure and death after hepatectomy. Ann Surg. 2005;242(6):824–8. discussion 8–9.
20. Paugam-Burtz C, Janny S, Delefosse D, Dahmani S, Dondero F, Mantz J, et al. Prospective validation of the "fifty–fifty" criteria as an early and accurate predictor of death after liver resection in intensive care unit patients. Ann Surg. 2009;249(1):124–8.
21. Jarnagin WR, Gonen M, Fong Y, DeMatteo RP, Ben-Porat L, Little S, et al. Improvement in perioperative outcome after hepatic resection: analysis of 1,803 consecutive cases over the past decade. Ann Surg. 2002;236(4):397–406, discussion 7.
22. Shirabe K, Shimada M, Gion T, Hasegawa H, Takenaka K, Utsunomiya T, et al. Postoperative liver failure after major hepatic resection for hepatocellular carcinoma in the modern era with special reference to remnant liver volume. J Am Coll Surg. 1999;188(3):304–9.
23. Ashwell G, Morell AG. The role of surface carbohydrates in the hepatic recognition and transport of circulating glycoproteins. Adv Enzymol Relat Areas Mol Biol. 1974;41:99–128.
24. Marshall JS, Green AM, Pensky J, Williams S, Zinn A, Carlson DM. Measurement of circulating desialylated glycoproteins and correlation with hepatocellular damage. J Clin Invest. 1974;54(3):555–62.
25. Sawamura T, Kawasato S, Shiozaki Y, Sameshima Y, Nakada H, Tashiro Y. Decrease of a hepatic binding protein specific for asialoglycoproteins with accumulation of serum asialoglycoproteins in galactosamine-treated rats. Gastroenterology. 1981;81(3):527–33.
26. Kwon AH, Ha-Kawa SK, Uetsuji S, Inoue T, Matsui Y, Kamiyama Y. Preoperative determination of the surgical procedure for hepatectomy using technetium-99m-galactosyl human serum albumin (99mTc-GSA) liver scintigraphy. Hepatology. 1997;25(2):426–9.
27. Sasaki N, Shiomi S, Iwata Y, Nishiguchi S, Kuroki T, Kawabe J, et al. Clinical usefulness of scintigraphy with 99mTc-galactosyl-human serum albumin for prognosis of cirrhosis of the liver. J Nucl Med. 1999;40(10):1652–6.
28. Kira T, Tomiguchi S, Takahashi M, Yoshimatsu S, Sagara K, Kurano R. Correlation of 99mTc-GSA hepatic scintigraphy with liver biopsies in patients with chronic active hepatitis type C. Radiat Med. 1999;17(2):125–30.
29. Seo Y, Mari C, Hasegawa BH. Technological development and advances in single-photon emission computed tomography/computed tomography. Semin Nucl Med. 2008;38(3):177–98.
30. Yumoto Y, Yagi T, Sato S, Nouso K, Kobayashi Y, Ohmoto M, et al. Preoperative estimation of remnant hepatic function using fusion images obtained by (99m)Tc-labelled galactosyl-human serum albumin liver scintigraphy and computed tomography. Br J Surg. 2010;97(6):934–44.
31. Bachellier P, Rosso E, Pessaux P, Oussoultzoglou E, Nobili C, Panaro F, et al. Risk factors for liver failure and mortality after hepatectomy associated with portal vein resection. Ann Surg. 2011;253(1):173–9.
32. Mathur AK, Ghaferi AA, Osborne NH, Pawlik TM, Campbell DA, Englesbe MJ, et al. Body mass index and adverse perioperative outcomes following hepatic resection. J Gastrointest Surg. 2010;14(8):1285–91.
33. Lynch RJ, Ranney DN, Shijie C, Lee DS, Samala N, Englesbe MJ. Obesity, surgical site infection, and outcome following renal transplantation. Ann Surg. 2009;250(6):1014–20.
34. Wei AC, Tung-Ping Poon R, Fan ST, Wong J. Risk factors for perioperative morbidity and mortality after extended hepatectomy for hepatocellular carcinoma. Br J Surg. 2003;90(1):33–41.
35. Takenaka K, Kanematsu T, Fukuzawa K, Sugimachi K. Can hepatic failure after surgery for hepatocellular carcinoma in cirrhotic patients be prevented? World J Surg. 1990;14(1):123–7.